Int. J. Electrochem. Sci., 14 **(2019)** 8544 – 8556, doi: 10.20964/2019.09.48

International Journal of ELECTROCHEMICAL SCIENCE
www.electrochemsci.org

Design, Fabrication and Investigation of Semitransparent Photo-thermoelectric Cell with Solar Water Collector for Energy Harvesting

Muhammad Mehran Bashir[1,*], *Khasan S Karimov*[1,2], *Jameel-Un Nabi*[1], *Noshin Fatima*[1], *Rashid Ali*[1]

[1] Ghulam Ishaq Khan Institute of Engineering Sciences and Technology, Topi-23640, District Swabi, KPK, Pakistan.
[2] Center for Innovative Development of Science and New Technologies of Academy of Sciences of Tajikistan, Dushanbe, 734025, Rudaki 33, Tajikistan.
[*]E-mail: mehran4gcu@gmail.com

Received: 12 May 2019/ *Accepted:* 8 July 2019 / *Published:* 31 July 2019

A semitransparent photo thermoelectric cell was designed and fabricated containing transparent glass plate on which the cylindrical thermoelectric cell was installed. The thermoelectric cell included a glass tube which was filled by the Bismuth Telluride (Bi_2Te_3) powder of n-type or p-type. Moreover, the gradient of temperature between two terminals of the thermoelectric cell was established by the effect of shading (glass plate shade or water collector shade) in the way of light and generated voltage was measured. The temperature dependence of the open circuit voltage and short circuit current, the gradient of temperature and position of shade and water collector were investigated. Range of light intensity was up to 150 W/m^2, the average temperature range of the thermoelectric cell was from 20 °C to 36 °C; gradient of temperature in the cell was in the range of 1-11 °C, the temperature of water in the collector increased from 20 °C to 30 °C. The electric and thermal efficiencies of the proposed semitransparent photo thermoelectric cell with solar water collector were equal to 0.02% and 39.5%, respectively. An investigation of the system was carried out where the thermoelectric cell was placed between shade and glass collector. Whilst shade covered the top and glass collector placed at the bottom. However, the current experimental setting provides lower thermal efficiency of the cell as compared to the initial setup, where a water collector was placed on the top of the thermoelectric cell. The proposed thermoelectric cell has twofold utilization, as a teaching aid for learning purposes and to build semitransparent windows. Further, these windows can produce electric power and heat while remaining semitransparent for natural light.

Keywords:semitransparent, photo-thermoelectric cell, energy harvesting, bismuth telluride, Seebeck coefficient, water collector.

1. INTRODUCTION

Recently, thermoelectric technology has been studied and developed for solar thermal applications in general and for solar thermoelectric generators (STEG) fabrication and investigation, in particular, [1]. In the 1950s , one of the first STEG having an efficiency of 3.5% was fabricated [2]. Presently several materials i.e. $AgPb_{18}SbTe_20$ and PbTe-SrTe doped with Na are reported to achieve a high figure of merit (ZT) equal to 2.2 [3, 4], they can be portable source of energy to have a beeter strategy in energy crisis. Moreover, a hybrid thermal thermoelectric generator (TEG) consisting of (TEG) and water collector was investigated [5]. One of the emerging technologies concerns solar photovoltaic thermoelectric (PV-TEG) hybrid technology which allows utilizing solar spectrum efficiently, improving the conversion efficiency, as reported in [6–11]. A flat-panel solar thermoelectric generator with high thermal concentration helped to achieve an efficiency of 4.6% at 1 kW/m^2 (AM 1.5G) condition, many folds higher as compared to earlier work [12]. The higher efficiency is due to, the use of nanostructured thermoelectric materials, selective solar absorbers, and high-quality concentrators, making this technology cost-effective for production of electric power from solar energy. In these devices Bi_2Te_3 for TEGs, dye-sensitized solar cells (DSSCs) and solar selective absorber (SSA) were used, achieving an overall efficiency of 13.8%. Moreover, when the gradient of temperature was 60 °C, power density was measured to be 12.8 mW [1]. The reported efficiency of STEG is further improved upto 15.9% provided the light intensity of 100 kWm^{-2} and hot terminal temperature would be 1000 °C [13]. Withal, a 100% increased in the efficiency is achieved if parameter ZT = 2 at 1500 °C. A cogeneration system was realized which contained STEG and solar hot water system. The system can produce either electric power or hot water. The peak efficiency of the Bi2Te3-based STEG is considered equal to 5% at AM 1.5G, the cost of the thermoelectric material is below 0.05 $/Wp [13].

An analytical analysis of concentrated solar thermoelectric generator was performed and variation of thermal absorber, selective absorber, concentration level and geometry of thermoelectric module were studied in [14].Experimental investigation of traditional materials like Bi_2Te_3 for thermoelectric applications having temperature range starting from 50 °C and ending at 200 °C was carried out and it was discovered that temperature difference has a linear and power has quadratic relation with efficiency of TEG device [15]. Efficiency surpassing 15% can be achieved by solar hybrid thermoelectric system proving the potential of application of solar energy for conversion to electric energy [16]. Usually, the STEGs have three basic components: the thermoelectric generator, the solar absorber and the heat exchanger or heat insulation. Nanomaterial based TEGs are of great interest due to their high temperature absorbance and thermal cavities providing path for further developments towards a cost effective model for high efficiency STEG technology. A cost-effective STEG system demands the synthesis and investigation of highly efficient thermoelectric materials at low cost and it could craft this technology ready for commercial applications. STEG systems can be used in concentrated and non-concentrated configuration. They have been employed in hybrid configurations with solar thermal and photovoltaic systems [17]. The key developments in the field of STEG are critically reviewed and analyzed by research community. A PV-TEG hybrid system consisting of non-tracking concentrator and glass lens was presented and two stage solar collector

system was realized in this work [18]. Moreover, the design, fabrication, and investigation of semitransparent thermoelectric cells based on graphene were done through detailed experiments in [19]. Furthermore, study of semitransparent thermoelectric cells on the base of Bi_2Te_3 and graphene was carried out in [20]. Combined photo-electric cell and thermoelectric generator for demonstrative purposes were described in [21]. Most of the STEGs were not semitransparent and conventionally without water collector. This paper presents a new setup of the design, fabrication, and investigation of the semitransparent photo-thermoelectric cell with solar water collector for solar energy capturing. This can be potentially used for window applications aiming for production of electric power, hot water and allowing natural light to penetrate inside a building.

2. EXPERIMENTAL

For the fabrication of semitransparent photo thermoelectric (SPTE) cell with solar water collector, the commercially available n-type Bismuth Telluride (n-Bi_2Te_3) and p-type Bismuth Telluride (p-Bi_2Te_3) in powder form were used. The average sizes of the powder particles of n-Bi_2Te_3 and p-Bi_2Te_3 were 11.56 µm and 12.15 µm, respectively. The Shimadzu centrifugal particle size analyzer SA-CP3 was used for the measurement of particle size. The measurement range of particle analyzer is 0.02 µm to 500 µm. Fig. 1 shows the X-Ray diffraction (XRD) graphs of the samples (n-Bi_2Te_3). The XRD of the samples was conducted with Philips PW1830 powder X-ray diffraction system. Scan mode Bragg-Brentano (θ-2θ) was used having Cu Kα radiation source at room temperature. In all diffractograms, the peaks of Bismuth Telluride (n-type) were observed at 2θ of 27.87° as shown in Fig. 1 and was found consistent with standard XRD data (PDF 051-0643). Fig. 2 represents the XRD graph of the sample (p- Bi_2Te_3). The peaks of Bismuth Telluride (p-type) were observed at 2θ of 28.11°. The standard XRD data (PDF 049-1713) was used to match the peaks. Fig. 3 shows a schematic diagram of the thermoelectric cell. Total length and diameter of the cell were equal to 3.5 cm and 0.7 cm, respectively. Fig. 4(a) shows the semitransparent photo thermoelectric (SPTE) cell with shade (side view). The dimension of the shade was equal to 1.5 cm × 3 cm and of the glass plate 3 cm × 4 cm. The thermoelectric cell was fixed on the glass plate. Fig. 4(b) shows the top view of the semitransparent photo-thermoelectric cell with shade. The uncovered and covered surfaces of the cell changed if the shade was moved in a horizontal direction along the longest axes of the thermoelectric cell. By this way, the gradient of temperature between two terminals of the thermoelectric cells and the generated output voltage was changed. Fig. 5(a) shows a semitransparent photo thermoelectric cell with a solar water collector (side view). The dimension of the water collector was 1 cm × 2 cm × 3 cm. Fig. 5(b) shows a semitransparent thermoelectric cell with a solar water collector (top view). The water collector can be moved in the horizontal direction along the longest axis of the thermoelectric cell.

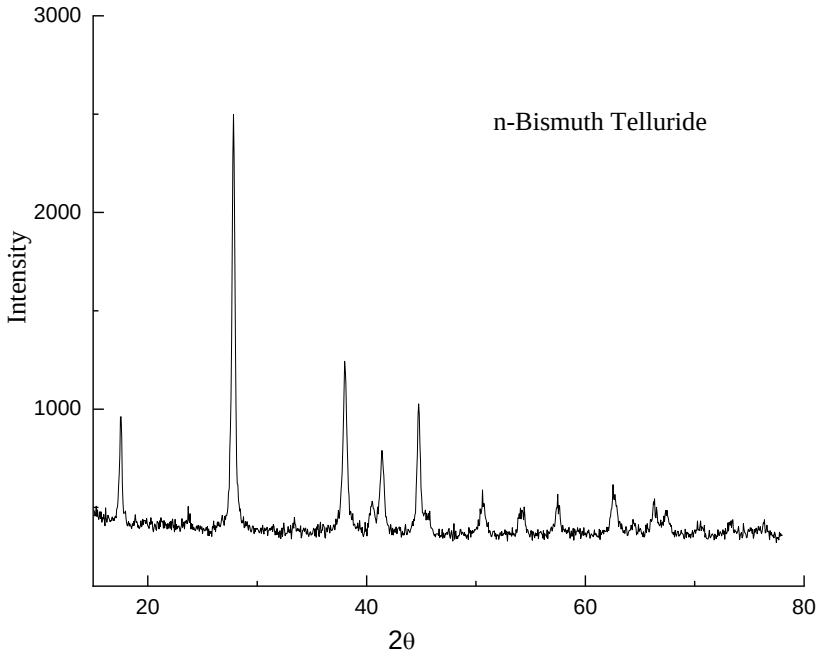

Figure 1. X-ray diffraction of bismuth telluride (n-type) powder sample

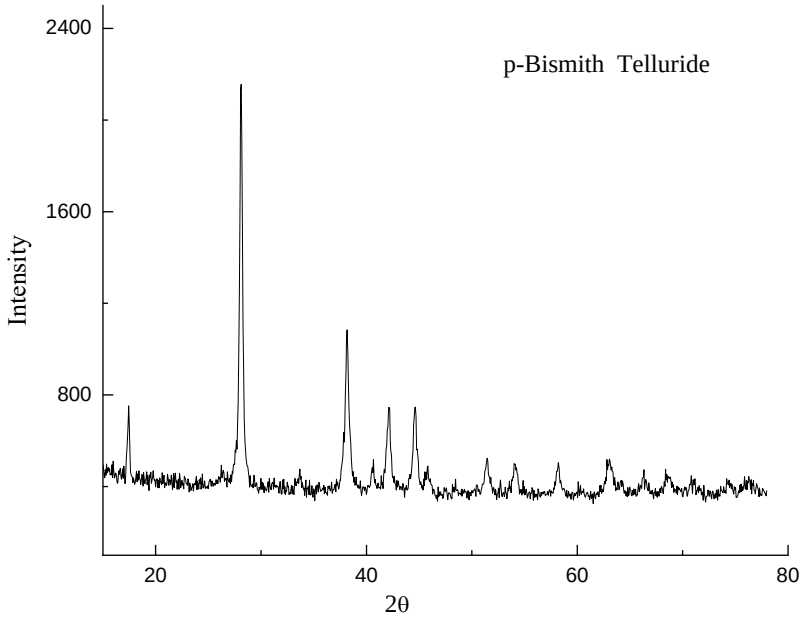

Figure 2. X-ray diffraction of bismuth telluride (p-type) powder sample

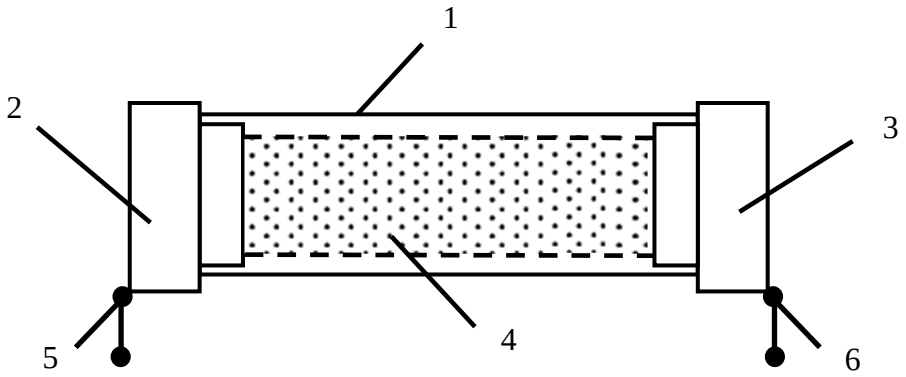

Figure 3. Photo-thermoelectric cell: glass cylindrical body (1), metallic electrodes (2 and 3), powder of n-Bi_2Te_3 or p-Bi_2Te_3, terminals-thermocouples (5 and 6)

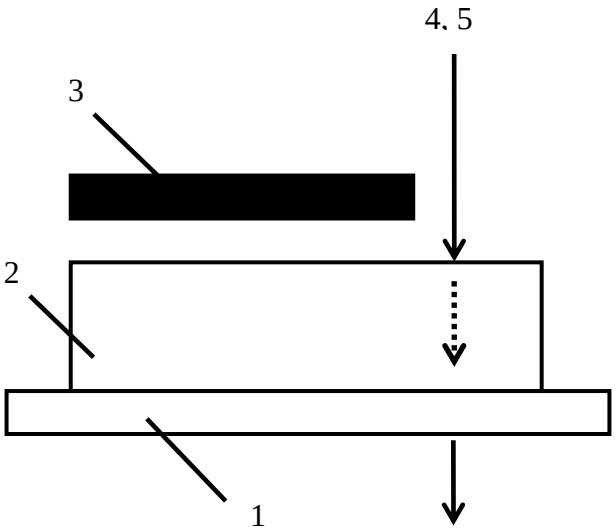

Figure 4.(a) Semitransparent Photo-thermoelectric cell (side view): glass plate (1), thermoelectric cell (2), shade (3), light beams (4 and 5).

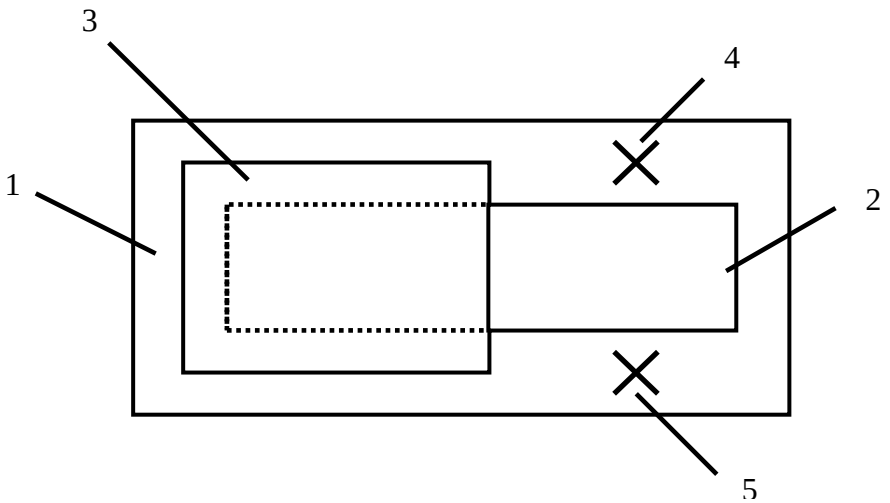

Figure 4.(b) Semitransparent Photo-thermoelectric cell (top view): glass plate (1), thermoelectric cell (2), shade (3), light beams (4 and 5).

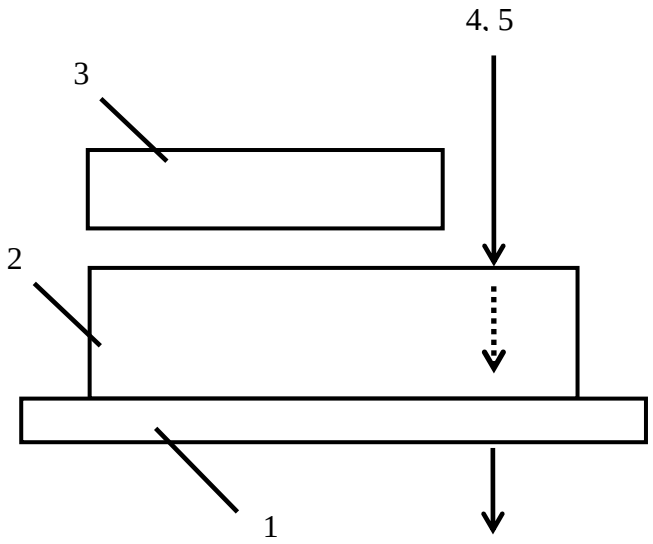

Figure 5.(a) Semitransparent Photo-thermoelectric cell (side view): glass plate (1), photo-thermoelectric cell (2), solar water collector (3), light beams (4 and 5).

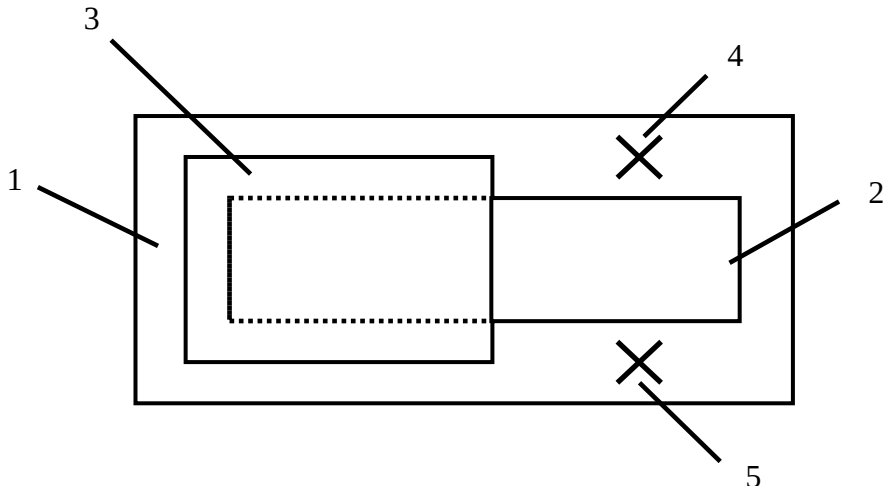

Figure 5.(b) Semitransparent Photo-thermoelectric cell (top view): glass plate (1), photo-thermoelectric cell (2), solar water collector (3), light beams (4 and 5).

The transparency of the semitransparent thermoelectric cell was estimated as a ratio of the light intensity at the surface of the un-shaded area of the thermoelectric cell to the intensity passed through the shaded area (glass shade or water collector) (in Fig. 4 and Fig. 5). The transparency was in the range of 42-65% depending on the position of the shade or water collector. We took into account the fact that the transparency of the water collector to visible light was equal to 95% and less transparent (30%) for infrared irradiation. The gradient of temperature between terminals of the thermoelectric cell was changed in the range of 1-11 °C; the average temperature was changed in the interval of 20-36 °C. A light source of filament lamp having a power rating of 200 W was used. Two multi-meters of FLUKE 87 with thermocouples were used for proper temperature and estimation of the gradient of the temperature measurements. Voltage and current were measured by multi-meters DT4253 and DT4252,

respectively. Devices LM-80 and LS-122-IR respectively measured intensities of visible light and infrared radiation.

3. RESULTSAND DISCUSSION

The fabricated SPTE cells with water collector were thoroughly investigated keeping in view the characterization aspects under different testing conditions. Initially, resistances of the Bi_2Te_3 samples were in the interval of 41-48Ω at room temperature.

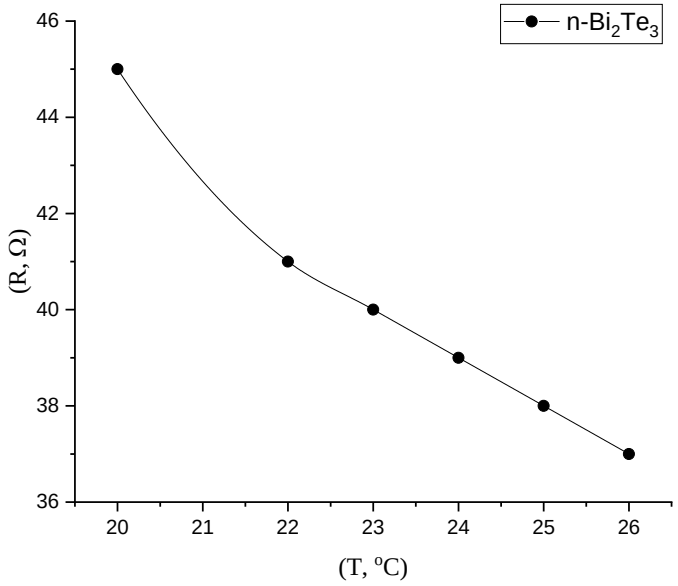

Figure 6. Variation of the resistance of the thermoelectric cell with respect to average temperature:

The resistance of fabricated SPTE cell gradually decreased with the increase of temperature. The following formula determines the temperature coefficient of the resistance (TCR):

$$\boldsymbol{TCR = \frac{\Delta R}{\Delta T R} 100\%} \qquad (\mathbf{1})$$

where ΔR, R, and ΔT are the change in resistance, the initial value of the resistance and gradient of temperature, respectively. TCR equal to (-2.96) %/°C was observed as per calculation is done. The electrical conductivity was equal to σ =0.10 Ω-1cm-1 at room temperature conditions. Fig. 6 indicates reliance on the resistance of the thermoelectric cell (of n-Bi_2Te_3 powder) on average temperature. Fig.7 depicts the variation of open-circuit voltage (V_{oc}) and short-circuit current (I_{sc}) on a gradient of temperature (ΔT) along the axis of the thermoelectric cell for the n- Bi_2Te_3 sample. The intensity of the illuminating at the thermoelectric cell was constant (150W/m^2). The gradient of temperature was established by shading of approximately half of the sample: the changing of the position of the shade along the sample axis allowed changing the gradient of temperature. From Fig. 7,

it can be clearly observed that as the gradient of temperature increased, the V_{oc} and I_{sc} increased as well as quasi-linearly.

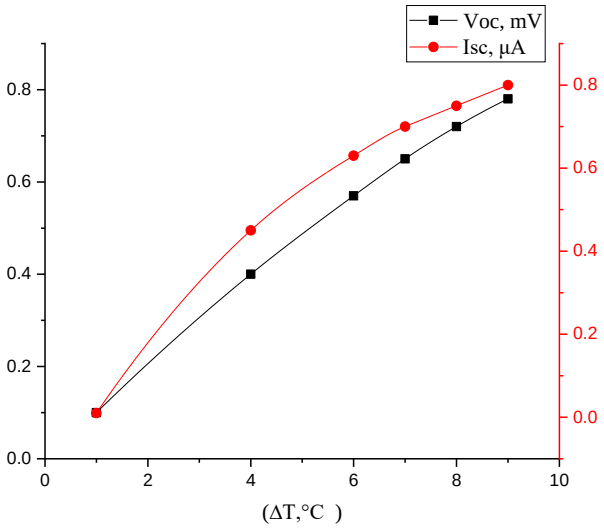

Figure 7. Variation of the open-circuit voltage (V_{oc}) and short-circuit current (I_{sc}) on the gradient of temperature (ΔT) along with the axis of the photo-thermoelectric cell with n-Bi_2Te_3 powder and photo-thermoelectric cell with shade.

Fig. 8 shows the dependence of V_{oc} and I_{sc} on ΔT for the n-Bi_2Te_3 sample where unlike to the previous case, the gradient of temperature was created by shading by use of solar water collector.It can be seen from Fig. 8 that as the gradient of temperature was increased the V_{oc} and I_{sc} were increased quasi-linearly.

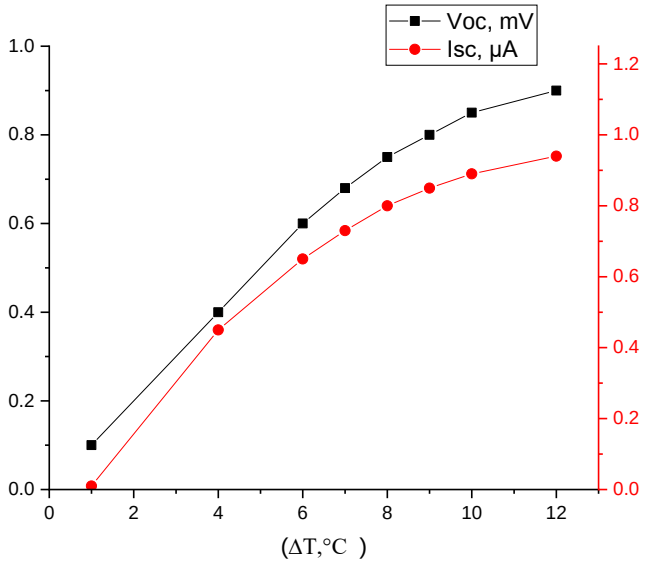

Figure 8. Variation of the open-circuit voltage (V_{oc}) and short-circuit current (I_{sc}) on the gradient of temperature (ΔT) along with the axis of the photo-thermoelectric cell with n-Bi_2Te_3 powder and photo-thermoelectric cell with solar water collector.

Fig. 9 shows the variation of V_{oc} and I_{sc} on ΔT for the p-Bi_2Te3. The water collector was used for the shading of the thermoelectric cell. In all graphs, the increase of the temperature gradient (ΔT) resulted in rise of the V_{oc} and I_{sc}.

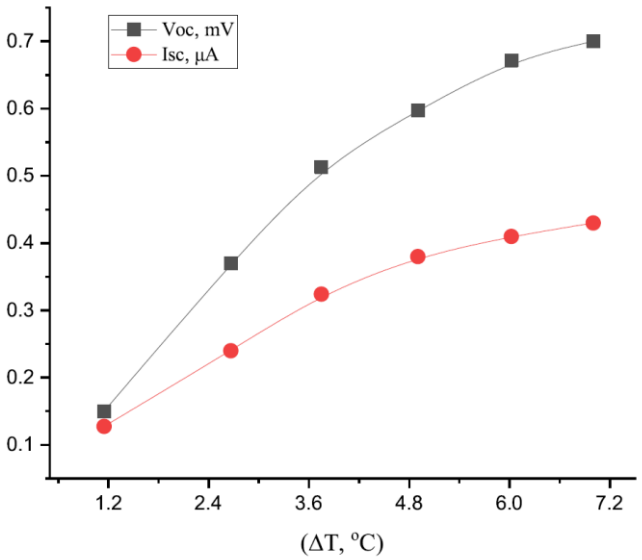

Figure 9. Variation of the open-circuit voltage (V_{oc}) and short-circuit current (I_{sc}) on the gradient of temperature (ΔT) along with the axis of the thermoelectric cell with p-Bi_2Te_3 powder and thermoelectric cell with solar water collector.

The thermoelectric sensitivity or Seebeck coefficient (α) as a ratio of open circuit voltage (thermoelectric voltage) increment (ΔV_{oc}) to increment of temperature (ΔT) is determined by the following expression

$$\boldsymbol{\alpha = \frac{\Delta V_{oc}}{\Delta T}} \qquad (\mathbf{2})$$

The thermopower or Seebeck coefficient is sensitive to impurities, mechanical properties and chemaical properties of materials. In case, a temperature gradient is applied across a thermeoelectric material, the charge carrier energy equilibrium is disturbed and average charge carrier energy varies resulting in transport of electron and phonons in the material and it is considered as main reason of Seebeck effect. Fermi Dirac Statistics are obeyed by electrons and resulting in photon participation in heat transport and electon in charge transport near the Fermi surface. It depends on the state of material and structutre of material too [22].

Analogously, thermoelectric sensitivity (β) for short circuit current (thermoelectric Current) can be calculated by:

$$\boldsymbol{\beta = \frac{\Delta I_{sc}}{\Delta T}} \qquad (\mathbf{3})$$

where ΔI_{sc} is an increment of short circuit current in Eq. 3. From data shown in Fig. 7, it was found that α= 85 µV/°C, β= 0.099 µA/°C for n-Bi_2Te_3 sample. By use of data of Fig. 8, it was calculated that α= 72µV/°C, β= 0.085µA/°C for n-Bi_2Te_3 sample. From the data of Fig. 9 for p-Bi_2Te_3 sample, it was determined that α= 92µV/°C, β= 0.052µA/°C. This shows that p-type samples gave a

higher value of α while lower value β of under the same conditions The heat (Q) required to raise the temperature of 12 g of water from 20 °C to 29 °C can be determined from the following equation:

$$\boldsymbol{Q = m\ x\ c\ x\ \Delta T} \qquad (\mathbf{4})$$

where m, c, and ΔT are the mass of the material, the specific heat capacity of the water (4.186 J/g°C) and the temperature change, respectively, in Eq. 4. The value of the obtained Q was 452 J. Fig. 10 represents the dependence of the temperature of water (in water collector) with respect to time. As the time of light falling on the solar water collector is increased , the temperature is increased due to heating effect of light energy as already experimentally obtained in [18]. Energy (E) of visible and infrared irradiation which over the transparent water collector can be estimated by the following way:

$$\boldsymbol{E_C = P\ x\ t} \qquad (\mathbf{5})$$

where P is the total power of visible and infrared irradiation, t is time during which water inside the collector was heated by irradiation (for $\boldsymbol{t}$=35 minutes, Fig. 10). The thermal efficiency (η_t) can be found as:

$$\boldsymbol{\eta_t = \frac{Q}{E}100\%} \qquad (\mathbf{6})$$

The thermal efficiency (η_t) comes out to be =35%. The electric power efficiency (η_e) of the thermoelectric cells was estimated as the ratio of the output electric power (P_e) of the thermoelectric cell to incident light power (P_i) (See Eq. 7).:

$$\boldsymbol{\eta_e = \frac{P_e}{P_i}\ 100\%} \qquad (\mathbf{7})$$

It was found that $\boldsymbol{\eta_e}$=0.02%.

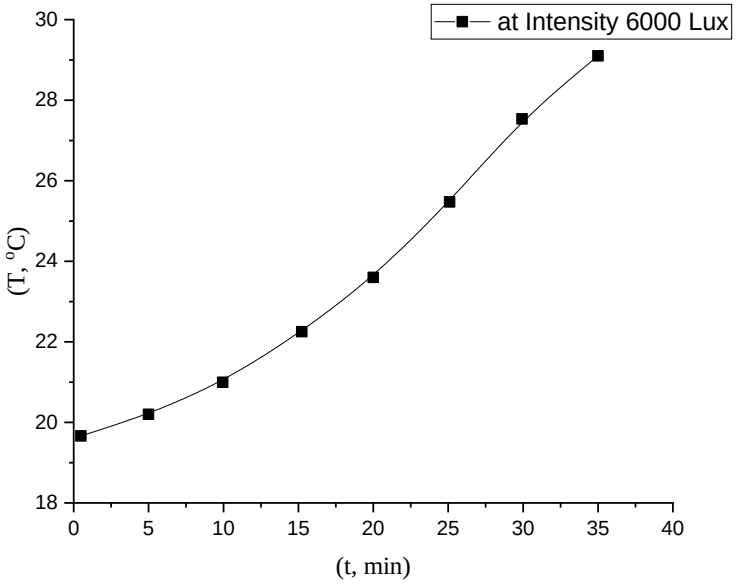

Figure 10. Variation of temperature of the water inside of solar water collector with respect to time

In order to increase the efficiency of the semitransparent thermoelectric cell, the gradient of temperature between its terminals should be maximum, for that a semitransparent plane reflector can be used.

Fig. 11 shows side view (a) and top view (b) of the semitransparent plane reflector with the built-in semitransparent thermoelectric cell. Peculiarities of this reflector are the following: (i) the reflector repeats the asymmetry of the thermoelectric unit; (ii) it possesses semitransparent reflecting side which allows reflecting part of the solar beam into the thermoelectric ; (iii) the part of the irradiation is reflected inside the building. Preliminary experiments showed that the reflection of the light intensity was in the range of 32-38%. The transmitted light intensity was 43-48%. These reflectors together with the semitransparent thermoelectric cell can be used for fabrication of the modules which can cover the whole window.

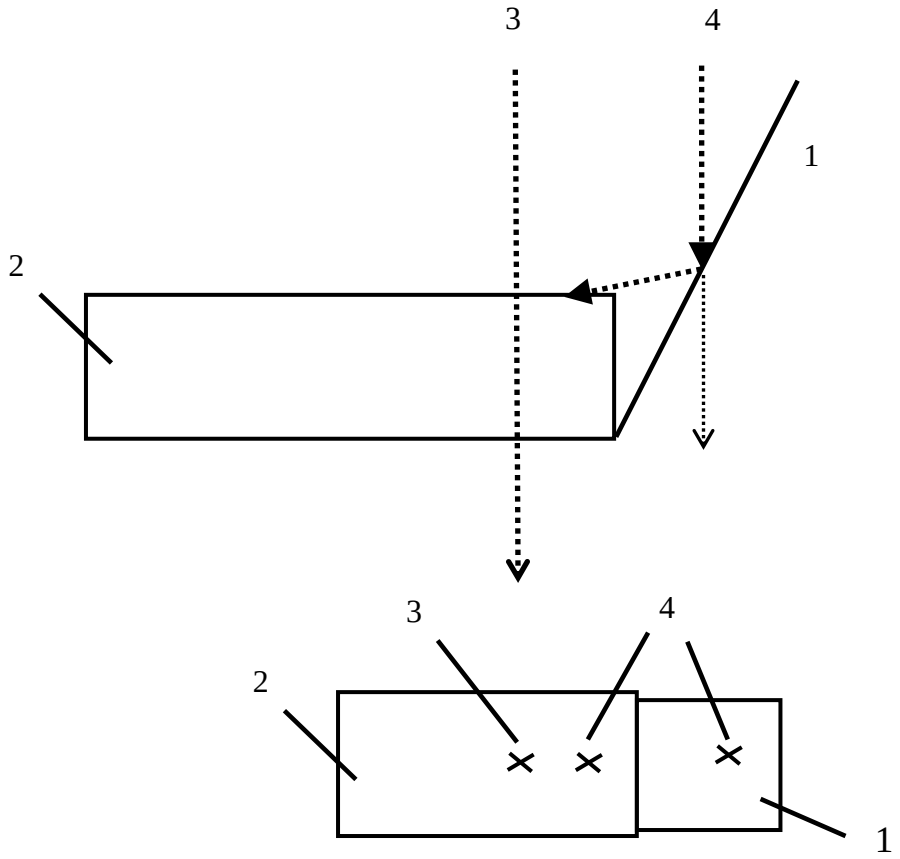

Figure 11. Side view (a) and top view (b) of the semitransparent reflector with the built-in semitransparent photo-thermoelectric cell.

Systematic investigations of the power generation by thermo-electric cells and Seebeck effect based on both inorganic and organic semiconductor materials were done in [22–25]. The thermo-electric efficiency (Z) can be determined by using the equation [26]:

$$\boldsymbol{Z = \frac{\alpha^2 \sigma}{K_{tot}}} \qquad (\mathbf{8})$$

where, $\boldsymbol{\alpha}$ is Seebeck coefficient, $\boldsymbol{\sigma}$ is electrical conductivity, and $\mathbf{K_{tot} = K_{el} + K_{ph}}$ is the sum of electron ($\mathbf{K_{el}}$) and phonon ($\mathbf{K_{ph}}$) thermal conductivities collectively known as total thermal

conductivity. The researchers showed immense interest in investigation of nanomaterials. In these materials, the efficiency of the thermoelectric generators increases as the phonon thermal conductivity ($\mathbf{K_{ph}}$) decreases.

Fabrication and investigation of the STEGs got significant achievements [23]: as the highest reported efficiency of STEGs was 5.2%. The concentrating STEGs have the potential to become a promising alternative solar energy technology [24–26]. The nano-structured Bi_2Te_3 and Sb_2Te_3 were synthesized and deposited on both sides of silk fabric to form columns of thermoelectric cells. For the connection of the thermocouples, the silver foils were used. The generator can easily convert thermal energy into electric energy, it was tested for twisting and bending of 100 cycles and after 30 minutes of walking the output data was collected. It proves that fabric as substrate can be used for thermoelectric power generators making it low cost and flexible [27]. Nanotubes based on p-type silicon were investigated for thermoelectric applications and thermo- electric effect was observed showing an improvement of five folds in figure of merit. At 700 °C, the power density was above 100 W/m^2 which is outstanding result for waste heat recovery market [28].

4. CONCLUSIONS

In this work, design, fabrication, and testing of the semitransparent photo thermoelectric cell containing a transparent glass plate over which the cylindrical thermoelectric cell, based on n-Bi_2Te_3 and p-Bi_2Te_3 powders, was undertaken. As per our information, for the first time, a water collector having high transparency (95%) for visible light and low transparency (30%) for infrared irradiation was integrated with the photo-thermoelectric cell. It played a double role: firstly, as a shade for development of the gradient of temperature along with the thermoelectric cell, and secondly for heating of the water. At present, intensive researches are going for fabrication and investigation of thermoelectric nanomaterials of the figure of merit (ZT) around 3 which allows increasing power efficiency up to an acceptable limit for practical applications, or close to Carnot efficiency (61.2%) was discussed in [28-29]. From results and discussed viewpoint, the constructed photo-thermoelectric cell can be used for further development of the semitransparent thermoelectric windows with overall higher efficiency due to the production of electric power, thermal power (water heating) and the illumination of the indoor space of the building. The generated power will be at least half of the energy of incident light.

ACKNOWLEDGEMENTS
The authors are thankful to the Ghulam Ishaq Khan Institute of Engineering Sciences and Technology and Higher Education Commission (HEC Project # 5345 under NRPU) of Pakistan for providing the facilities and support for this work.

References

1. P. Sundarraj, D. Maity, S. S. Roy and R. A. Taylor, *RSC Adv.*, 4 (2014) 46860–46874.

2. M. Telkes, *J. Appl. Phys.*, 25 (1954) 765–777.
3. K. F. Hsu, S. Loo, F. Guo, W. Chen, J. S. Dyck, C. Uher, T. Hogan, E. K. Polychroniadis and M. G. Kanatzidis, *Science*, 303 (2004) 818–821.
4. K. Biswas, J. He, I. D. Blum, C.-I. Wu, T. P. Hogan, D. N. Seidman, V. P. Dravid and M. G. Kanatzidis, *Nature*, 489 (2012) 414.
5. M. Zhang, L. Miao, Y. P. Kang, S. Tanemura, C. A. Fisher, G. Xu, C. X. Li and G. Z. Fan, *Appl. Energy*, 109 (2013) 51–59.
6. Y. Vorobiev, J. González-Hernández, P. Vorobiev and L. Bulat, *Sol. Energy*, 80 (2006) 170–176.
7. D. Kraemer, L. Hu, A. Muto, X. Chen, G. Chen and M. Chiesa, *Appl. Phys. Lett.*, 92 (2008) 243503.
8. Y. Li, S. Witharana, H. Cao, M. Lasfargues, Y. Huang and Y. Ding, *Particuology*, 15 (2014) 39–44.
9. T. Liao, B. Lin and Z. Yang, *Int. J. Therm. Sci.*, 77 (2014) 158–164.
10. M. Fisac, F. X. Villasevil and A. M. López, *J. Power Sources*, 252 (2014) 264–269.
11. X. Zhang, X. Zhao, S. Smith, J. Xu and X. Yu, *Renew. Sustain. Energy Rev.*, 16 (2012) 599–617.
12. D. Kraemer, B. Poudel, H.-P. Feng, J. C. Caylor, B. Yu, X. Yan, Y. Ma, X. Wang, D. Wang and A. Muto, *Nat. Mater.*, 10 (2011) 532.
13. D. Kraemer, K. McEnaney, M. Chiesa and G. Chen, *Sol. Energy*, 86 (2012) 1338–1350.
14. L. L. Baranowski, G. J. Snyder and E. S. Toberer, *Energy Environ. Sci.*, 5 (2012) 9055–9067.
15. E. A. Chávez-Urbiola, Y. V. Vorobiev and L. P. Bulat, *Sol. Energy*, 86 (2012) 369–378.
16. C. Maurer, T. Pflug, P. Di Lauro, J. Hafner, F. Knez, S. Jordan, M. Hermann and T. E. Kuhn, *Energy Procedia*, 30 (2012) 1035–1041.
17. M. L. Olsen, E. L. Warren, P. A. Parilla, E. S. Toberer, C. E. Kennedy, G. J. Snyder, S. A. Firdosy, B. Nesmith, A. Zakutayev and A. Goodrich, *Energy Procedia*, 49 (2014) 1460–1469.
18. Kh. S. Karimov and Z. Ahmad, *Appl. Phys. A*, 124 (2018) 857.
19. M. T. S. Chani, K. S. Karimov, J. Nabi, M. Hashim, I. Kiran and A. M. Asiri, *Int. J. Electrochem. Sci.*, 13 (2018) 11777–11786.
20. N. Fatima, M. Riaz, K. S. Karimov, A. Kh. M, M. Ilolov and J. Nabi, *Int. J. Appl. Fund. Reseach*, 3 (2018) 26–30.
21. K. Skarimov, Z. Baig, S. A. Moiz, A. Khan, K. Khmedov and U. Rao, *Acad. J. Scient. Research*, (2017) 12.
22. Y. Zhang, Y.J. Heo, M. Park and S.J. Park, *Polymers*, 11 (2019) 1-22.
23. D. Kraemer, Q. Jie, K. McEnaney, F. Cao, W. Liu, L. A. Weinstein, J. Loomis, Z. Ren and G. Chen, *Nat. Energy*, 1 (2016) 16153.
24. M. Sumino, K. Harada, M. Ikeda, S. Tanaka, K. Miyazaki and C. Adachi, *Appl. Phys. Lett.*, 99 (2011) 188.
25. S. B. Riffat and X. Ma, *Appl. Therm. Eng.*, 23 (2003) 913–935.
26. L. E. Bell, *Science*, 321 (2008) 1457–1461.
27. Z. Lu, H. Zhang, C. Mao and C. M. Li, *Appl. Energy*, 164 (2016) 57–63.
28. A. Morata, M. Pacios, G. Gadea, C. Flox, D. Cadavid, A. Cabot and A. Tarancón, *Nat. Commun.*, 9 (2018) 4759.
29. X. Zhang and L.-D. Zhao, *J. Materiomics*, 1 (2015) 92–105.
30. S. Yazdani and M. T. Pettes, *Nanotechnology*, 29 (2018) 432001.